Aerospace Science and Technology 54 (2016) 218–228

Contents lists available at ScienceDirect

Aerospace Science and Technology

www.elsevier.com/locate/aescte

# Adaptive neural network-based satellite attitude control in the presence of CMG uncertainty

W. MacKunis [a,*], F. Leve [b], P.M. Patre [c], N. Fitz-Coy [d], W.E. Dixon [d]

[a] Physical Sciences Department, Embry-Riddle Aeronautical University, Daytona Beach, FL 32114, United States
[b] Air Force Research Laboratory, Kirtland Air Force Base, Albuquerque, NM 87117, United States
[c] TE Connectivity, Advanced Manufacturing Technologies Sector, Harrisburg, PA 17111, United States
[d] Mechanical and Aerospace Engineering Department, University of Florida, Gainesville, FL 32611-6250, United States

ARTICLE INFO

*Article history:*
Received 9 November 2015
Received in revised form 18 April 2016
Accepted 19 April 2016
Available online 26 April 2016

ABSTRACT

An attitude tracking controller is developed for control moment gyroscope (CMG)-actuated satellites, which is shown to achieve accurate attitude tracking in the presence of unmodeled external disturbance torques, parametric uncertainty, and nonlinear CMG disturbances. Since the disturbances/uncertainties do not all satisfy the typical linear-in-the-parameters (LP) assumption, a neural network (NN) is included in the control development. The innovation of the result is the development of a Lyapunov-based design/analysis that indicates exponential convergence to an arbitrarily small domain. The result is obtained despite the characteristics of the uncertainty; the nonvanishing disturbance terms; and the fact that the control input is premultiplied by a non-square, time-varying, nonlinear, uncertain matrix. In addition to the Lyapunov-based analysis, experimental results demonstrate the performance of the developed controller.



## 0. Introduction

The design of attitude control systems (ACS) for satellites is complicated due to external disturbances, parametric uncertainty, and nonlinearities, which inevitably exist in the corresponding plant dynamics. ACS design for satellites can be further complicated by parametric uncertainty and disturbances present in the dynamics of the control actuators. Actuator disturbances can be especially significant in smaller satellites (small-sats), since the inertia of the control actuator (e.g., control moment gyroscopes (CMGs)) can be comparable to that of the satellite itself. Standard adaptive control approaches can be utilized to compensate for constant parametric uncertainty in the plant and actuator dynamics [1]. Sliding mode control [2], $H_\infty$ [3,4], and extended Kalman Filter-based [5] approaches have been shown to be effective in compensating for external disturbances in ACS. However, most standard approaches (e.g., see [2–4]) assume a known dynamic model for the external disturbances (e.g., solar radiation pressure, gravity gradient torque, magnetic attitude disturbance, atmospheric drag). To improve control flexibility, intelligent control methods can be employed to develop accurate ACS for a more general class of systems containing multiple sources of unknown, unmodeled nonlinear disturbances.

To achieve attitude control in the presence of parametric uncertainties, adaptive control techniques have been investigated by several researchers. In [6], an output feedback model reference adaptive controller is developed for spacecraft rendezvous and docking problems. The adaptive controller in [6] accommodates for inertia uncertainty in the momentum wheel actuator dynamics; however, no electromechanical disturbances were assumed to be present in the actuator model. A quaternion-based, full-state feedback attitude tracking controller was designed in [7] for a rigid satellite with unknown inertia. An adaptive control law is designed in [8], which incorporates a velocity-generating filter from attitude measurements. The controller in [8] is shown to achieve asymptotic convergence of the attitude and angular velocity tracking errors despite uncertainty in the satellite inertia, but it assumes no dynamic uncertainty in the control torque. The aforementioned adaptive control methods have been shown to achieve attitude control for their respective control tasks, under the assumption that the parametric uncertainty is linear-in-the-parameters (i.e., LP uncertainty). For more general classes of dynamic

* Corresponding author.
*E-mail addresses:* william.mackunis@erau.edu (W. MacKunis), frederick.leve@us.af.mil (F. Leve), parag.patre@gmail.com (P.M. Patre), nfc@ufl.edu (N. Fitz-Coy), wdixon@ufl.edu (W.E. Dixon).

http://dx.doi.org/10.1016/j.ast.2016.04.022
1270-9638/

systems with ill-defined or completely unknown mathematical models, data-based approaches can be utilized [9]. Data-based approaches have been shown to be effective in fault diagnosis and process monitoring and control for industrial applications, for example (e.g., see [10]). However, intelligent control methods can offer a practical alternative in engineering applications, for which partial knowledge of the system dynamics can be leveraged.

To cope with disturbances and nonlinearities that do not obey the linear-in-the-parameters assumption (i.e., non-LP), fuzzy control or NN-based control methods are often utilized [11–17]. In [15], an approximation-based adaptive fuzzy control scheme is presented, which is shown to compensate for unmodeled dynamics for a class of nonlinear strict-feedback systems. The scheme in [15] utilizes fuzzy logic systems to approximate unknown nonlinearities, and Lyapunov–Krasovskii functionals are employed to compensate for time-delays. In [12], an attitude control approach based on the radial basis function neural network (RBFNN) is developed. The satellite dynamic model utilized in [12] includes no disturbances in the reaction wheel actuators. Another NN attitude controller is presented in [14], which utilizes NNs to approximate the parametric uncertainties and nonlinearities present in the system dynamics. The NN is used in [14] to re-optimize a Single Network Adaptive Critic, or SNAC-based optimal controller, designed a priori for the nominal system. In [11], a NN attitude controller is developed based on a simplified nonlinear model of the Space Station Freedom. The dynamic model for the space station considered in [11] is simplified by assuming small roll/yaw attitude errors and small products of inertia. The attitude controller in [11] demonstrates the capability of the NN to adaptively compensate for varying inertia characteristics. The NN controllers presented in [11] and [14] are developed under the assumption that a control torque can be directly applied to the system, and no uncertainty is present in the actuators. The aforementioned fuzzy logic and NN-based control methods have been shown to be an effective means to compensate for unmodeled nonlinearities in dynamic systems. However, the attitude control approach presented in this paper focuses on addressing the challenge of rejecting unmodeled disturbances while simultaneously compensating for uncertain CMG actuator dynamics. To achieve this, the proposed attitude control method employs an innovative amalgamation of adaptive control and online NN-based estimation methods.

For applications involving small-sats, the assumption that a control torque can be directly applied to the system may not be valid, because the control torques are generated by actuators (e.g., CMGs) which have uncertain dynamics. These actuator uncertainties can have a more pronounced effect for pico- and nano-class satellites, where the CMGs are of significant size in comparison to the satellite itself. For small-sats, the inertia of the CMGs is comparable to the overall inertia of the satellite, so the motion of the CMG actuators can alter the overall inertia of the satellite. The resulting time variation in the satellite inertia manifests itself as a disturbance torque in the dynamic model. While this source of disturbance is often assumed to be negligible in some satellite dynamic models, it can be significant in the dynamics for small-sats. Furthermore, the torque-producing capacity of CMGs can deteriorate over time due to bearing degradation and increased friction in the gimbals. Electromechanical disturbances (e.g., tachometer ripple, motor cogging, motor back electromotive forces (BEMF), commutation or switching errors, and other electrical errors) can also hinder CMG performance [18]. The presence of these mechanical and electromechanical factors in the CMG actuators causes significant challenges in designing ACS for small-sats using CMG actuators.

An adaptive NN-based attitude tracking controller is developed in this paper for CMG-actuated satellites, which is capable of achieving attitude control in the presence of unmodeled external disturbances in addition to disturbances resulting from CMG actuator dynamics. Since the external disturbances are assumed to be unknown and non-LP, standard adaptive control techniques cannot be applied to compensate for their effects. By exploiting the function approximation property of NNs, these unknown nonlinearities are estimated, and the NN estimate is used in the control law to compensate for their effects. While a NN could be utilized to compensate for both the LP and non-LP uncertainty, NN-based estimation has lower performance than adaptive estimation for structured (i.e., LP) uncertainty. A contribution of the control method presented here is innovative algebraic manipulation in the tracking error system development, which enables the design of a control law that efficiently amalgamates adaptive and NN-based estimation to reject external non-LP disturbances while simultaneously compensating for LP uncertainty in the CMG actuators. The controller is applicable to CMG-actuated satellites of any size, but the control structure is designed with an emphasis on compensating for disturbances that are characteristic to small-sats. To that end, the controller is designed to compensate for time-varying satellite inertia, CMG parametric uncertainty, and nonlinear, non-LP external disturbance torques. Electromechanical uncertainties in the gimbal servo loop (i.e., uncertain loop gains and rotor inertias) are also assumed to be present in the CMG actuators. Some of the challenges encountered in the control design are that the control input (i.e., CMG gimbal angular rate) is premultiplied by a non-square, time-varying, nonlinear, uncertain matrix due to electromechanical uncertainties. Furthermore, due to the small size of the satellite considered in this development, the motion of the CMGs causes significant time-variation in the satellite inertia characteristics. The time-variation of the satellite inertia manifests itself as a nonlinear disturbance torque in the satellite dynamic model, which is handled via innovative algebraic manipulation in the error system development along with a Lyapunov-based adaptive update law. In addition, experimental results are provided, which demonstrate the performance of the controller in an attitude regulation task.

## 1. Dynamic model and properties

The dynamics of a spacecraft modeled as a rigid body and actuated by CMGs can be expressed as [19]

$$J\dot{\omega} = -\omega^{\times} J\omega + \tau_{cmg} - \dot{J}\omega + \tau_d. \tag{1}$$

In (1), $J(\delta) \in \mathbb{R}^{3\times 3}$ represents the positive definite, symmetric satellite inertia matrix that is a function of the CMG gimbal angular position vector $\delta(t) \in \mathbb{R}^4$. The dimension of the gimbal angle vector $\delta(t)$ is based on the assumption that the CMG cluster contains four single gimbal CMGs (SGCMGs); however, the control design presented here is applicable in any scenario in which the number of SGCMGs is greater than or equal to the number of rotational degrees of freedom (i.e., three). The inertia matrix $J(\delta)$ satisfies the inequality

$$\lambda_{\min}\{J\}\|\xi\|^2 \leq \xi^T J\xi \leq \lambda_{\max}\{J\}\|\xi\|^2 \quad \forall\, \xi \in \mathbb{R}^n, \tag{2}$$

where $\|\cdot\|$ represents the standard Euclidean norm, and $\lambda_{\min}\{J\}$, $\lambda_{\max}\{J\} \in \mathbb{R}$ are the minimum and maximum eigenvalues of $J(\delta)$, respectively. Also in (1), $\omega(t) \in \mathbb{R}^3$ denotes the angular velocity of the satellite body-fixed frame $\mathcal{F}$ with respect to an inertial frame $\mathcal{I}$

expressed in $\mathcal{F}$, and $\tau_{cmg}(t) \in \mathbb{R}^3$ denotes the internal torque (control torque) generated via a CMG cluster consisting of four SGCMGs. Also in (1), the term $\dot{J}(t)\omega(t)$ represents the torque produced by the time variation of the satellite inertia matrix due to the motion of the CMGs, and the notation $\zeta^{\times}\ \forall\ \zeta \in \mathbb{R}^3$ denotes the skew-symmetric matrix equivalent to a vector cross product. In (1), $\tau_d(t) \in \mathbb{R}^3$ denotes a general, unmodeled, nonlinear disturbance torque.

**Remark 1.** In (1), the term $\tau_d(t)$ could represent external disturbances due to solar radiation pressure, gravity gradient torque, magnetic interactions, aerodynamic drag, mounting misalignment, and/or a general unmodeled, nonlinear external disturbance torque. While dynamic models have been developed for certain commonly known disturbance sources [2–4,20,21], the ACS design presented here assumes that the dynamic model for the external disturbance is completely unknown. The disturbance torques listed will have a more pronounced effect depending on the satellite, its inertia, and its orbit regime. A NN is utilized along with a Lyapunov-based adaptive law to estimate and compensate for the effects of the disturbance.

The control torque generated from the CMG cluster including tachometer disturbances can be modeled as [18]

$$\tau_{cmg} = -\left(\dot{h}_{cmg} + \omega^{\times} h_{cmg}\right) + AT_d, \tag{3}$$

where $A(\delta) \in \mathbb{R}^{3\times 4}$ denotes a measurable Jacobian matrix, which relates the four SGCMG gimbal-fixed frames to the three coordinate axes of the satellite body-fixed frame. The Jacobian matrix is explicitly defined as

$$A(\delta) \triangleq \begin{bmatrix} -\sin\gamma\sin\delta_1 & -\cos\delta_2 & \sin\gamma\sin\delta_2 & \cos\delta_4 \\ \cos\delta_1 & -\sin\gamma\sin\delta_2 & -\cos\delta_2 & \sin\gamma\sin\delta_4 \\ -\cos\gamma\sin\delta_1 & \cos\gamma\sin\delta_2 & -\cos\gamma\sin\delta_3 & -\cos\gamma\sin\delta_4 \end{bmatrix}. \tag{4}$$

Since the Jacobian matrix $A(\delta)$ contains only bounded trigonometric terms, it can be upper bounded as:

$$\|A(\delta)\|_{i\infty} \leq \zeta_0, \tag{5}$$

where $\zeta_0 \in \mathbb{R}$ is a known positive bounding constant, and $\|\cdot\|_{i\infty}$ denotes the induced infinity norm of a matrix. Also in (3), $h_{cmg}(t) \in \mathbb{R}^3$ represents the angular momentum of the CMG cluster, and $\dot{h}_{cmg}(t)$ is modeled as

$$\dot{h}_{cmg} = hA\dot{\delta}, \tag{6}$$

where $h \in \mathbb{R}$ represents the constant angular momentum of each SGCMG expressed in the gimbal-fixed frame (i.e., $h$ is the same for all four SGCMGs). In (6), $\dot{\delta} \triangleq \begin{bmatrix} \dot{\delta}_1 & \dot{\delta}_2 & \dot{\delta}_3 & \dot{\delta}_4 \end{bmatrix}^T \in \mathbb{R}^4$ denotes the CMG gimbal angular rate control input, where $\dot{\delta}_i(t) \in \mathbb{R}\ \forall\ i = 1,2,3,4$ denotes the angular rate of the $i$th SGCMG gimbal. The term $T_d\left(\delta, \dot{\delta}\right) \in \mathbb{R}^4$ in (3) represents torques in the gimbal axes due to tachometer disturbances. For tachometers consisting of a stator and a rotating magnetic rotor, signal errors can result as the voltage signal produced by the rotating magnet passes the windings of the stator. The errors resulting from these tachometer disturbances manifest themselves as sinusoidal voltage disturbances that generally range from low to high frequencies. Mathematically, tachometer disturbances can be expressed as [18]

$$T_d \triangleq K_G E_d \dot{\delta}, \tag{7}$$

where $K_G \in \mathbb{R}^{4\times 4}$ denotes a diagonal matrix of uncertain, constant forward loop gains for the four SGCMG gimbal loops, and $E_d(\delta) = diag\{E_{d1}(\delta_1),\ E_{d2}(\delta_2),\ E_{d3}(\delta_3),\ E_{d4}(\delta_4)\}$ is a matrix of disturbance voltages in the four gimbals, where $E_{di}(\delta_i)$, for $i = 1,2,3,4$, are functions of the $i$th gimbal angle defined as

$$E_{di} \triangleq \sum_{n=1}^{10} \left\{ \frac{1}{n}\sin(n\delta_i) + \frac{1}{n+1}\cos(n\delta_i) \right\}. \tag{8}$$

The CMG torque expression in (3) does not explicitly include gimbal acceleration terms or dynamics between $\delta(t)$ and $\dot{\delta}(t)$, but these effects are assumed to be included with the other bounded uncertainties, which contribute to the ultimate bound on the tracking error.

## 2. Kinematic model

The rotational kinematics of the rigid-body satellite can be expressed as [7]

$$\dot{q}_v = \frac{1}{2}\left(q_v^{\times}\omega + q_0\omega\right), \quad \dot{q}_0 = -\frac{1}{2}q_v^T\omega. \tag{9}$$

In (9), $q_v(t) \in \mathbb{R}^3$ and $q_0(t) \in \mathbb{R}$ denote the vector and scalar parts, respectively, of the quaternion $q(t) \triangleq \{q_0(t), q_v(t)\} \in \mathbb{R}\times\mathbb{R}^3$ that describes the orientation of the body-fixed frame $\mathcal{F}$ with respect to $\mathcal{I}$, subject to the constraint

$$q_v^T q_v + q_0^2 = 1. \tag{10}$$

In the subsequent analysis, $q_d(t) \triangleq \{q_{0d}(t), q_{vd}(t)\} \in \mathbb{R}\times\mathbb{R}^3$ denotes the unit quaternion that describes the orientation of the desired body-fixed frame $\mathcal{F}_d$ with respect to $\mathcal{I}$. Rotation matrices that bring $\mathcal{I}$ onto $\mathcal{F}$ and $\mathcal{I}$ onto $\mathcal{F}_d$, denoted by $R(q_v, q_0) \in SO(3)$ and $R_d(q_{vd}, q_{0d}) \in SO(3)$, respectively, can be developed using standard quaternion kinematics (see [22] for details). The subsequent analysis is based on the assumption that $q_{0d}(t)$, $q_{vd}(t)$, and their first three time derivatives are bounded for all time. This assumption ensures that the desired angular velocity $\omega_d(t) \in \mathbb{R}^3$ and its first two time derivatives are bounded for all time.

## 3. Control objective

The objective in this paper is to develop a gimbal velocity controller to enable the attitude of $\mathcal{F}$ to track the attitude of $\mathcal{F}_d$. To quantify the objective, an attitude tracking error denoted by $\tilde{R}(e_v, e_0) \in \mathbb{R}^{3\times 3}$ is defined that brings $\mathcal{F}_d$ onto $\mathcal{F}$ as

$$\tilde{R} \triangleq R R_d^T = \left(e_0^2 - e_v^T e_v\right) I_3 + 2 e_v e_v^T - 2 e_0 e_v^{\times}, \tag{11}$$

where $e(t) \triangleq \{e_0(t), e_v(t)\} \in \mathbb{R} \times \mathbb{R}^3$ denotes the quaternion tracking error, and $I_3$ is the $3 \times 3$ identity matrix. Since the actual and desired angular velocity vectors $\omega(t)$ and $\omega_d(t)$ are defined in the reference frames $\mathcal{F}$ and $\mathcal{F}_d$, respectively, $\omega_d(t)$ must be transformed to the frame $\mathcal{F}$ so that the angular velocity tracking error between $\omega(t)$ and $\omega_d(t)$ can be defined in $\mathcal{F}$. To this end, (11) is used to define the angular velocity of $\mathcal{F}$ with respect to $\mathcal{F}_d$ expressed in $\mathcal{F}$, denoted by $\tilde{\omega}(t) \in R^3$, as

$$\tilde{\omega} \triangleq \omega - \tilde{R}\omega_d. \tag{12}$$

To facilitate the subsequent control design, an auxiliary control signal, denoted by $r(t) \in \mathbb{R}^3$, is defined as

$$r \triangleq \omega - \tilde{R}\omega_d + \alpha e_v, \tag{13}$$

where $\alpha \in \mathbb{R}$ is a positive, constant control gain. After substituting (13) into (12), the angular velocity tracking error can be expressed as

$$\tilde{\omega} = r - \alpha e_v. \tag{14}$$

Motivation for the design of $r(t)$ is based on the subsequent Lyapunov-based stability analysis and the fact that (12) can be used to express the open-loop quaternion tracking error as

$$\dot{e}_v = \frac{1}{2}\left(e_v^{\times} + e_0 I\right)\tilde{\omega}, \qquad \dot{e}_0 = -\frac{1}{2} e_v^T \tilde{\omega}. \tag{15}$$

From the definitions of the quaternion tracking error variables, the following constraint holds [7]:

$$e_v^T e_v + e_0^2 = 1. \tag{16}$$

Thus, (11) can be used to conclude that if $\|e_v(t)\| \to 0$, $\tilde{R} \to I_3$, and the control objective will be achieved.

**Assumption 1.** The general disturbance $\tau_d(t) \in \mathbb{R}^3$ (see Equation (1)) is an unknown nonlinear function of the measurable states $q_v(t)$, $q_0(t)$, $\dot{q}_v(t)$, $\dot{q}_0(t)$, and $\omega(t)$. Examples of known disturbance sources satisfying this functional dependence include gravity gradient torque, aerodynamic drag [20], mounting misalignment [4], and solar radiation pressure [21]. In the following control development, the disturbance $\tau_d(t)$ is assumed to be an unknown, unmeasurable function, which is attenuated using a feedforward NN-based estimate.

## 4. Control development

The contribution of this paper is development, which shows how adaptive estimation can be amalgamated with NN-based function approximation to attenuate unmodeled external disturbances while simultaneously compensating for CMG actuator disturbances. To achieve the result, innovative algebraic manipulation is performed in the tracking error system development, resulting in a mathematically advantageous segregation of the structured (LP) actuator uncertainty from the unstructured (non-LP) external disturbances. This strategy in the error system development facilitates the design of a novel control structure, which effectively combines the benefits of adaptive estimation with NN-based approximation to achieve accurate attitude tracking control for a general class of systems with unmodeled dynamics.

### 4.1. Open-loop error system

The open-loop dynamics for $r(t)$ can be determined by taking the time derivative of (13) and premultiplying the resulting expression by $J(\delta)$ as

$$J\dot{r} = J\dot{\omega} + J\tilde{\omega}^{\times}\tilde{R}\omega_d - J\tilde{R}\dot{\omega}_d + J\alpha\dot{e}_v, \tag{17}$$

where the fact that $\dot{\tilde{R}} = -\tilde{\omega}^{\times}\tilde{R}$ was utilized. After using the dynamic model given in (1) and the expression for $\tau_{cmg}(t)$ given in (3), the expression in (17) can be rewritten as

$$J\dot{r} = f - \Omega_0\dot{\delta} - hA\dot{\delta} + AK_G E_d\dot{\delta} - \omega^{\times} h_{cmg} - \frac{1}{2}\dot{J}r, \tag{18}$$

where (6), (7), (13), and (15) were utilized. In (18), $\Omega_0(r,\ e_v,\ e_0,\ \omega_d,\ \delta,\ t) \in \mathbb{R}^{3\times 4}$ denotes an uncertain auxiliary matrix, which is defined via the parameterization[1]

$$\Omega_0\dot{\delta} = \left(\frac{d}{dt}J(\delta)\right)\left(\frac{1}{2}r + \tilde{R}\omega_d - \alpha e_v\right). \tag{19}$$

[1] A detailed derivation of the linear parameterization in (19) can be found in the appendix.

**Remark 2.** The linear parameterization presented in Equation (19) is one of the salient features of the innovation presented here of the proposed method. This enables us to effectively segregate the LP terms from the non-LP terms in the error system development to combine adaptive and NN-based feedforward terms in the control law and achieve a very advantageous combination of NN and adaptive control techniques.

Also in (18), the unknown nonlinear function $f(r,\ q_v,\ q_0,\ e_v,\ e_0,\ \omega,\ \omega_d,\ \dot{\omega}_d,\ \delta,\ t) \in \mathbb{R}^3$ is defined as

$$f \triangleq -\omega^{\times} J\omega + J\tilde{\omega}^{\times}\tilde{R}\omega_d - J\tilde{R}\dot{\omega}_d + \frac{1}{2}J\alpha\left(e_v^{\times} + e_0 I\right)\tilde{\omega} + \tau_d. \tag{20}$$

Although the variable inertia in $J(\delta)$ is LP through the constant but unknown gimbal inertia, it is included in the NN here to compensate for a more general source of unmodeled dynamics. For example, it may be possible for the gimbals to be flexible and for the dynamic balance (e.g., alignment of the rotor-axis to the gimbal axis) to be influenced by such flexible effects.

To facilitate the subsequent Lyapunov-based adaptive control design, the terms in (18) containing parametric uncertainty are linearly parameterized as

$$Y_1\theta_1 \triangleq \Omega_0\dot{\delta} - AK_G E_d\dot{\delta}, \tag{21}$$

where $Y_1(r,\ e_v,\ e_0,\ \omega_d,\ \delta,\ \dot{\delta},\ t) \in \mathbb{R}^{3\times p_1}$ is a known, measurable regression matrix, and $\theta_1 \in \mathbb{R}^{p_1}$ is a vector of $p_1$ unknown constants. One of the control design challenges for the open-loop system in (18) is that the control input $\dot{\delta}(t)$ is premultiplied by a nonsquare, uncertain time-varying matrix. To address this issue, an estimate of the uncertainty in (21), denoted by $\hat{\Omega}_1(t) \in \mathbb{R}^{3\times 4}$, is defined via

$$\hat{\Omega}_1\dot{\delta} = Y_1\hat{\theta}_1, \tag{22}$$

where $\hat{\theta}_1(t) \in \mathbb{R}^{p_1}$ is a subsequently designed estimate for the parametric uncertainty in $\Omega_1(r,\ e_v,\ e_0,\ \omega_d,\ \delta,\ t)$. Based on (21) and (22), (18) can be rewritten as

$$J\dot{r} = f - B\dot{\delta} - \omega^{\times}h_{cmg} - \frac{1}{2}\dot{J}r - Y_1\tilde{\theta}_1, \tag{23}$$

where $B(\delta, t) \in \mathbb{R}^{3\times 4}$ is defined as[2]

$$B \triangleq hA + \hat{\Omega}_1, \tag{24}$$

and the parameter estimate mismatch $\tilde{\theta}_1(t) \in \mathbb{R}^{p_1}$ is defined as

$$\tilde{\theta}_1 \triangleq \theta_1 - \hat{\theta}_1. \tag{25}$$

## 5. Feedforward NN estimation

The open-loop tracking error dynamics in (23) contains structured (LP) actuator uncertainty in addition to unstructured (non-LP) uncertainty due to unmodeled external disturbances. An adaptive control method will be utilized in the subsequent control design, where we exploit the known structure of the actuator uncertainty. However, the uncertainty due to disturbances is unstructured, and this motivates the need for additional compensation. To this end, NN-based function approximation will also be incorporated in the control design.

NN-based estimation methods are well suited for dynamic models containing unstructured uncertainties as in (1). The main feature that empowers NN-based controllers is the universal approximation property. A NN will be utilized to approximate the unknown nonlinear function $f$ defined in (20). By utilizing a feedforward NN-based estimate, the control law can be designed to achieve accurate attitude tracking control for a general class of systems, where multiple sources of unmodeled external disturbances might be present. The use of a NN can thus enable reliable attitude tracking control for a satellite over a wide range of uncertain and potentially adversarial operating conditions.

Let $\mathbb{S}$ be a compact simply connected set of $\mathbb{R}^{N_1+1}$. Let $\mathbb{C}^n(\mathbb{S})$ be defined as the space where $f : \mathbb{S} \to \mathbb{R}^n$ is continuous. The universal approximation property states that there exist weights and thresholds such that the function $f(x) \in \mathbb{C}^n(\mathbb{S})$ can be represented by a three-layer NN as [23]

$$f(x) = W^T\sigma\left(V^T x\right) + \varepsilon(x). \tag{26}$$

In (26), $V \in \mathbb{R}^{(N_1+1)\times N_2}$ and $W \in \mathbb{R}^{(N_2+1)\times n}$ are bounded constant ideal weight matrices for the first-to-second and second-to-third layers, respectively, where $N_1$ is the number of neurons in the input layer, $N_2$ is the number of neurons in the hidden layer, and $n$ is the number of neurons in the third layer. Based on (20), the measurable NN input vector $x(t) \in \mathbb{R}^{N_1+1}$ is defined as

$$x(t) \triangleq \begin{bmatrix} 1 & r^T(t) & q_v^T(t) & q_0^T(t) & e_v^T(t) & e_0(t) & \omega^T(t) & \omega_d^T(t) & \dot{\omega}_d^T(t) & g^T(\delta) \end{bmatrix}^T, \tag{27}$$

where $g(\cdot) \in \mathbb{R}^4$ denotes a vector of bounded trigonometric functions (e.g., $\sin(\cdot)$ or $\cos(\cdot)$).[3] The activation function in (26) is denoted by $\sigma(\cdot) : \mathbb{R}^{N_1+1} \to \mathbb{R}^{N_2+1}$, and $\varepsilon(x) : \mathbb{R}^{N_1+1} \to \mathbb{R}^n$ is the functional reconstruction error.[4]

[2] The purpose of the feedforward estimate $\hat{\Omega}_1(t)$ is to compensate for parametric input uncertainty, not to add rank to the original Jacobian matrix $A(\delta)$.

[3] The parallel axis theorem can be used to prove that the gimbal angle $\delta(t)$ enters into the dynamic equations of motion through direction cosine matrices, thus $\delta(t)$ only appears in the unknown function $f(x)$ within bounded trigonometric functions.

[4] The value for $N_1$ is based on the size of the input vector $x(t)$, and the number of hidden layer weights $N_2$ is selected to yield the desired NN approximation accuracy.

**Remark 3.** If $\varepsilon = 0$, then $f(x)$ is in the functional range of the NN. In general, for any positive constant real number $\varepsilon_{b1} > 0$, $f(x)$ is within $\varepsilon_{b1}$ of the NN range if there exist finite hidden neurons $N_2$ and constant weights so that for all inputs in the compact set $\mathbb{S}$, the approximation holds with $\|\varepsilon(x)\| < \varepsilon_{b1}$. The Stone–Weierstrass theorem indicates that any sufficiently smooth function can be approximated by a suitably large network. Therefore, the fact that the approximation error $\varepsilon(x)$ is bounded follows from the Universal Approximation Property of NNs. Application of the Stone–Weierstrass theorem requires that $x(t) \in \mathbb{S}$. From (13) and (27), if $r(t)$ is a member of some compact set $\mathbb{S}_r \subset \mathbb{S}$, then $x(t) \in \mathbb{S}$. The subsequent stability proof shows that if $r(0)$ is bounded, then $r(t) \in \mathbb{S}_r$.

Based on (26), the typical three-layer NN approximation for $f(x)$ is given as [23]

$$\hat{f}(x) = \hat{W}^T \sigma\left(\hat{V}^T x\right), \tag{28}$$

where $\hat{V}(t) \in \mathbb{R}^{(N_1+1)\times N_2}$ and $\hat{W}(t) \in \mathbb{R}^{(N_2+1)\times n}$ are subsequently designed estimates of the ideal weight matrices. The estimate mismatch for the ideal weight matrices, denoted by $\tilde{V}(t) \in \mathbb{R}^{(N_1+1)\times N_2}$ and $\tilde{W}(t) \in \mathbb{R}^{(N_2+1)\times n}$, are defined as

$$\tilde{V} \triangleq V - \hat{V} \qquad \tilde{W} \triangleq W - \hat{W}, \tag{29}$$

and the mismatch for the hidden layer output error for a given $x(t)$, denoted by $\tilde{\sigma}(x) \in \mathbb{R}^{(N_2+1)}$, is defined as

$$\tilde{\sigma} \triangleq \sigma - \hat{\sigma} = \sigma\left(V^T x\right) - \sigma\left(\hat{V}^T x\right). \tag{30}$$

The neural network estimate has several properties that facilitate the subsequent development. These properties are described as follows.

**Property 1** *(Taylor series approximation).* The Taylor series expansion for $\sigma\left(V^T x\right)$ for a given $x$ may be written as [23]

$$\sigma\left(V^T x\right) = \sigma\left(\hat{V}^T x\right) + \sigma'\left(\hat{V}^T x\right)\tilde{V}^T x + o\left(\tilde{V}^T x\right)^2, \tag{31}$$

where $\sigma'\left(\hat{V}^T x\right) \equiv d\sigma\left(V^T x\right)/d\left(V^T x\right)|_{V^T x = \hat{V}^T x}$, and $o\left(\tilde{V}^T x\right)^2$ denotes the higher order terms. After substituting (31) into (30), the following expression can be obtained:

$$\tilde{\sigma} = \hat{\sigma}'\tilde{V}^T x + o\left(\tilde{V}^T x\right)^2, \tag{32}$$

where $\hat{\sigma}' \triangleq \sigma'\left(\hat{V}^T x\right)$.

**Assumption 2** *(Boundedness of the ideal weights).* The ideal weights are assumed to exist and be bounded by known positive values so that

$$\|V\|_F^2 = tr\left(V^T V\right) \le \bar{V}_B, \quad \|W\|_F^2 = tr\left(W^T W\right) \le \bar{W}_B \tag{33}$$

where $\|\cdot\|_F$ is the Frobenius norm of a matrix, and $tr(\cdot)$ is the trace of a matrix.

The desired angular velocity is assumed to be bounded such that

$$\left\| \left[\, \omega_d^T(t) \;\; \dot{\omega}_d^T(t) \,\right]^T \right\| \le \zeta_d, \tag{34}$$

where $\zeta_d$ is a known bounding constant. It follows that for each time $t$, $x(t)$ can be bounded as

$$\|x\| \le c_1 + c_2 \|r\|, \tag{35}$$

where $c_1$ and $c_2$ are computable constants.

### 5.1. Closed-loop error system

Based on the open-loop dynamics in (23) and the following stability analysis, the control input is designed as

$$\dot{\delta} = B^{\#}\left[\hat{f} - \omega^{\times} h_{cmg} + K_v r + k_n r + e_v\right], \tag{36}$$

where $K_v, k_n \in \mathbb{R}$ denote positive control gains (i.e., $k_n$ is a nonlinear damping term). Also in (36), $B^{\#}(\delta, t) \in \mathbb{R}^{4\times 3}$ denotes a pseudoinverse of $B(\delta, t)$ defined as [24,25]

$$B^{\#} = B^T\left(BB^T + \zeta I_3\right)^{-1}. \tag{37}$$

In (37), $\zeta(\delta, t) \in \mathbb{R}$ denotes a singularity avoidance parameter, which is used to avoid singularities in the $B$ matrix. For example, Nakamura et al. [24] designed $\zeta(\delta, t)$ as

$$\zeta(\delta, t) \triangleq \epsilon_0 \exp\left[-\det\left(BB^T\right)\right], \tag{38}$$

so that $\zeta(\delta, t)$ is negligible when $BB^T$ is nonsingular but increases to the constant parameter $\epsilon_0 \in \mathbb{R}$ as the singularity is approached. Since the matrix in Eq. (24) is not the Jacobian of the CMG array (i.e., due to the uncertainty estimate), the pseudoinverse in Eq. (37) is utilized to ensure control effectiveness rather than singularity avoidance. Singularities in the CMG configuration matrix $A$ are not explicitly accounted for, but our preliminary results demonstrate the capability of the control law to avoid singularities by successfully maneuvering out of a singularity present from controller initialization. Also in (36), the feedforward NN component, denoted as $\hat{f}(t) \in \mathbb{R}^n$, is defined as in (28), where the state vector $x(t) \in \mathbb{R}^{N_1+1}$ is defined in (27). The estimates of the NN weights in (28) are generated on-line (there is no off-line learning phase) as [26]

$$\dot{\hat{W}} \triangleq proj\left(\Gamma_1\left(\hat{\sigma} r^T - \hat{\sigma}' \hat{V}^T x r^T\right)\right) \tag{39}$$

$$\dot{\hat{V}} \triangleq proj\left(\Gamma_2 x r^T \left(\hat{\sigma}'^T \hat{W}\right)^T\right), \tag{40}$$

where $\Gamma_1 \in \mathbb{R}^{(N_2+1)\times(N_2+1)}$, $\Gamma_2 \in \mathbb{R}^{(N_1+1)\times(N_1+1)}$ are constant, positive definite, symmetric control gain matrices.

The closed-loop tracking error system can be developed by substituting (36) into (23) as

$$J\dot{r} = -\frac{1}{2}\dot{J}r + \tilde{f} - Y_1\tilde{\theta}_1 - K_v r - k_n r - e_v, \tag{41}$$

where $\tilde{f}(x) \in \mathbb{R}^3$ represents a function estimation error vector defined as $\tilde{f} \triangleq f - \hat{f}$. Based on (41) and the subsequent stability analysis, the parameter estimate $\hat{\theta}_1(t)$ is designed as

$$\dot{\hat{\theta}}_1 = proj(-\Gamma_3 Y_1^T r), \tag{42}$$

where $\Gamma_3 \in \mathbb{R}^{p_1 \times p_1}$ denotes a constant, positive-definite, diagonal adaptation gain matrix.

**Remark 4.** The function $proj(\cdot)$ in (39), (40), and (42) denotes a standard algorithm, which ensures that the following inequalities are satisfied (for further details, see [27,28]):

$$\underline{V}_{ij} \le \hat{V}_{ij} \le \bar{V}_{ij}, \qquad \underline{W}_{kl} \le \hat{W}_{kl} \le \bar{W}_{kl}, \qquad \underline{\theta}_{1m} \le \hat{\theta}_{1m} \le \bar{\theta}_{1m}, \tag{43}$$

where $\underline{V}_{ij}$, $\bar{V}_{ij}$, $\underline{W}_{kl}$, $\bar{W}_{kl}$, $\underline{\theta}_{1m}$, $\bar{\theta}_{1m} \in \mathbb{R}$ denote known, constant lower and upper bounds of $\hat{V}_{ij}(t)\ \forall\ i = 1, \ldots, (N_1+1)$, $\forall\ j = 1, \ldots, N_2$; $\hat{W}_{kl}(t)\ \forall\ k = 1, \ldots, (N_2+1)$, $\forall\ l = 1, \ldots, n$; and $\hat{\theta}_{1m}(t)\ \forall\ m = 1, \ldots, p_1$, respectively.

**Remark 5.** To determine $\hat{W}(t)$, $\hat{V}(t)$, and $\hat{\theta}_1(t)$, the adaptation laws in (39), (40), and (42) assume the availability of angular position and velocity measurements only.

After using (26), (28), and the Taylor series approximation described in (31) and (32), the closed-loop error system in (41) can be expressed as

$$J\dot{r} = -\frac{1}{2}\dot{J}r + w - K_v r - k_n r - e_v - Y_1\tilde{\theta}_1 + \tilde{W}^T\left(\hat{\sigma} + \hat{\sigma}'\hat{V}^T x\right) + \hat{W}^T\hat{\sigma}'\tilde{V}^T x, \tag{44}$$

where (30) was used, and $w(t) \in \mathbb{R}^3$ is defined as

$$w = \tilde{W}^T\hat{\sigma}'V^T x + W^T o\left(\tilde{V}^T x\right)^2 + \varepsilon(x). \tag{45}$$

For notational convenience, let the matrix containing all NN weights be defined as $Z \triangleq diag\{W, V\}$.

Based on the assumption that the NN approximation property holds for all $x(t)$ in a compact set (the subsequent stability proof illustrates that $x(t)$ remains in a compact set), the NN reconstruction error $\varepsilon(x)$ can be upper bounded as $\|\varepsilon(x)\| \le \varepsilon_{b1}$. Therefore, $\varepsilon(x)$ and the higher order terms in the Taylor series expansion of $f(x)$ can be treated as disturbances in the error system. Moreover, these disturbances can be upper bounded as

$$\|w(t)\| \le c_3 + c_4 Z_M \|r\|, \tag{46}$$

where $c_3$, $c_4 \in \mathbb{R}$ are known positive constants. Also in (46), $Z_M \in \mathbb{R}$ is a bounding constant that satisfies $\|Z\|_F \le Z_M$. To facilitate the subsequent analysis, the control gain $K_v$ in (36) is selected as

$$K_v > c_4 Z_M. \tag{47}$$

## 6. Stability analysis

**Theorem 1.** *The adaptive controller of (22), (24), (28), (36)–(40), and (42) ensures bounded attitude tracking in the sense that*

$$\|e_v(t)\| \le \varepsilon_0 \exp\{-\varepsilon_1 t\} + \varepsilon_2, \tag{48}$$

*where $\varepsilon_0$, $\varepsilon_1$, $\varepsilon_2 \in \mathbb{R}$ denote positive bounding constants.*

**Proof.** Let $V_L\left(e_0, e_v, r, \hat{W}, \hat{V}, \hat{\theta}, t\right) \in \mathbb{R}$ be defined as the nonnegative function

$$V_L(t) \triangleq e_v^T e_v + (1-e_0)^2 + \frac{1}{2} r^T J r + \frac{1}{2} tr\left(\tilde{W}^T \Gamma_1^{-1} \tilde{W}\right) + \frac{1}{2} tr\left(\tilde{V}^T \Gamma_2^{-1} \tilde{V}\right) + \frac{1}{2} \tilde{\theta}_1^T \Gamma_3^{-1} \tilde{\theta}_1. \tag{49}$$

Based on (2), (25), (39), (40), and (43), the Lyapunov function candidate (49) can be upper and lower bounded as

$$\lambda_1 \|y\|^2 + c_7 \leq V_L(t) \leq \lambda_2 \|y\|^2 + c_8, \tag{50}$$

where $y(t) \in R^6$ is defined as

$$y \triangleq \left[\, e_v^T \;\; r^T \,\right]^T, \tag{51}$$

and $\lambda_1$, $\lambda_2$, $c_7$, $c_8 \in \mathbb{R}$ are known positive bounding constants. After using (14), (15), (44), and the tuning rules given in (39), (40), and (42), the time derivative of $V_L(t)$ can be expressed as

$$\dot{V}_L = -\alpha e_v^T e_v + r^T \left(w - K_v r - k_n r\right), \tag{52}$$

where the fact that $e_v^T e_v^{\times} \tilde{\omega} = 0$ was utilized. After substituting the upper bound for $\|w\|$ given in (46) and utilizing the inequality in (47), the expression in (52) can be upper bounded as

$$\dot{V}_L(t) \leq -\lambda_3 \|y\|^2 - k_n \|r\|^2 + c_3 \|r\|, \tag{53}$$

where $\lambda_3 \in \mathbb{R}$ is a positive bounding constant. Completing the squares in (53) yields

$$\dot{V}_L(t) \leq -\lambda_3 \|y\|^2 + \frac{c_3^2}{4k_n}. \tag{54}$$

Based on (50), (54) can be expressed as

$$\dot{V}_L(t) \leq -\frac{\lambda_3}{\lambda_2} V_L(t) + \varepsilon_0, \tag{55}$$

where $\varepsilon_0 \triangleq \frac{c_3^2}{4k_n} + \frac{\lambda_3 c_8}{\lambda_2}$. The linear differential inequality in (55) can be solved as

$$V_L(t) \leq \exp\left\{-\frac{\lambda_3}{\lambda_2} t\right\} V_L(0) + \varepsilon_0 \frac{\lambda_2}{\lambda_3} \left(1 - \exp\left\{-\frac{\lambda_3}{\lambda_2} t\right\}\right). \tag{56}$$

The expressions in (49), (50), and (56) can be used to conclude that $r(t) \in \mathcal{L}_\infty$. Thus, from (14) and (51), $\tilde{\omega}(t)$, $y(t) \in \mathcal{L}_\infty$, and (13) can be used to conclude that $\omega(t) \in \mathcal{L}_\infty$. The open-loop quaternion tracking error in (15) can be used to show that $\dot{e}_v(t)$, $\dot{e}_0(t) \in \mathcal{L}_\infty$. Hence, (24), (28), (36), (39), and (40) can be used to prove that the control input $\dot{\delta}(t) \in \mathcal{L}_\infty$. Standard signal chasing arguments can then be utilized to prove that all remaining signals remain bounded during closed-loop operation. The inequalities in (50) can be used along with (56) to conclude that

$$\|y\|^2 \leq \left(\frac{\lambda_2 \|y(0)\|^2 + c_8}{\lambda_1}\right) \exp\left\{-\frac{\lambda_3}{\lambda_2} t\right\} + \left(\frac{\lambda_2 c_3^2}{4k_n \lambda_3 \lambda_1} + \frac{c_8 - c_7}{\lambda_1}\right) < \varepsilon_3(y(0)), \tag{57}$$

where $\varepsilon_3$ is a positive constant. The result in (48) can now be directly obtained from (51) and (57). Also, from (51), $r(t)$ is contained for all times $t \geq 0$ in a compact set $\mathbb{S}_r = \{\, y(t) \,|\, \|y(t)\| < \varepsilon_3(y(0))\}$. According to the Weierstrass approximation theorem, given any NN approximation error bound there exist some number of neurons such that $\sup_{y \in \mathbb{S}_r} \|\varepsilon(x)\| < \varepsilon_{b1}$. □

## 7. Experiment

To test the validity of the controller developed in (36), (39), (40), and (42), an experiment was performed using the University of Florida Spacecraft Orientation Buoyancy Experimental Kiosk (SOBEK) CMG test bed.

The test bed uses four single gimbal CMGs in an orthogonal pyramid configuration. The inclination of the pyramid walls is $\gamma = 54.74°$. The numerical values of the dynamic parameters for the SOBEK test bed (i.e., $h$, $J_0$, $r_i$, ${}^{gi}J_{gi}$ $\forall\, i = 1, \ldots, 4$) are readily available. The CMG electromechanical disturbances are assumed to be modeled as in (7), and the gimbal servo loop gains $K_{Gi}$ $\forall\, i = 1, \ldots, 4$ are assumed to be unknown and are not used in the control law.

A Phasespace motion capture system takes range measurements from LEDs located on the SOBEK ACS and calculates the quaternion position of the ACS. Due to the test bed setup, it was impractical to use onboard gyros for angular velocity measurements. Instead, the angular rates of the ACS were estimated via differentiation of the quaternion position measurements. The experimental results were achieved using estimates of $\delta(t)$ that were obtained by numerically integrating the commanded gimbal rate. In the absence of angular velocity measurements, the experiment tests attitude regulation instead of tracking.

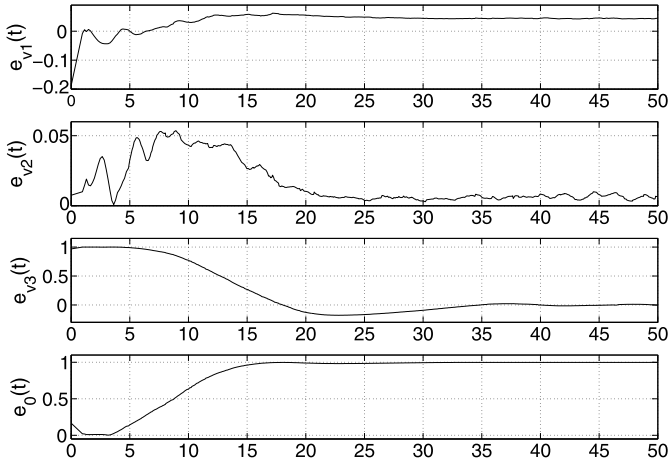


**Fig. 1.** Quaternion tracking error during closed-loop controller operation of experimental test bed [dimensionless].

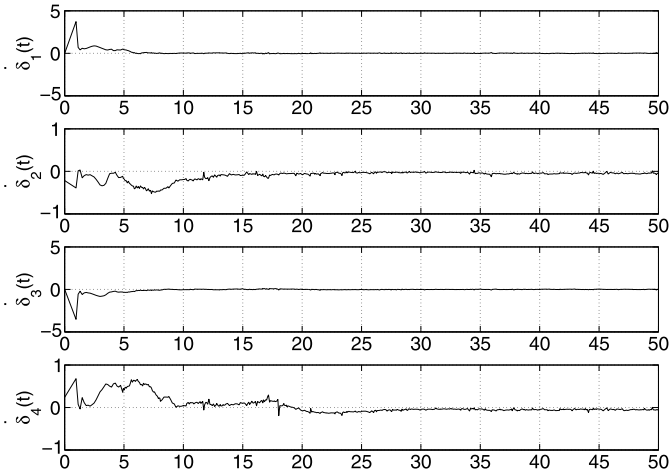


**Fig. 2.** Control input gimbal angular rates [deg/sec] used in experiment during closed-loop controller operation.

### 7.1. Summary of results

The goal of the experiment was to perform an attitude maneuver from an initial quaternion orientation of $q(0) = [-0.15,\ 0.01,\ 0.98,\ 0.15]^T$ to a desired quaternion orientation of $q_d = [0,\ 0,\ 0,\ 1]^T$. The initial gimbal angles were set to a singular configuration of $\delta(0) = [0,\ 0,\ 0,\ 0]^T$ deg. The initialization of the gimbal configuration to a singularity tests a worst-case scenario because maneuvering out of a singularity present from controller initialization is more difficult than it would be if the singularity were encountered within the maneuver. Figs. 1–2 summarize the experimental results achieved by implementing the controller in (36), (37)–(40), and (42) with control gains selected as follows:

$$\begin{array}{ccc} K_v = 0.2 & k_n = 0.7 & K_Z = 0.05 \\ \kappa = 2.5 & \alpha = 2 & \epsilon_0 = 0.2 \\ \Gamma_1 = 10.2 I_{21} & \Gamma_2 = 5 I_{21} & \Gamma_3 = 0.1 I_6 \end{array}$$

and the adaptive and NN weight estimates were initialized as

$$\hat{\theta}(0) = 0_{6\times 1} \qquad \hat{W}(0) = 0_{21\times 3} \tag{58}$$
$$\hat{V}_{ij}(0) = 0.1 \sin(\text{rand}) \qquad \forall\, i = 1, ..., 25,\ \forall\, j = 1, ..., 10.$$

Fig. 1 shows the quaternion attitude error $e(t)$ versus time. Fig. 2 shows the control input gimbal rates.

The experimental results are based on the gimbal rate control law defined in Equations (28) and (36)–(40). The control law includes a nonlinear damping feedback term and feedforward adaptive estimates of uncertain parameters and of the ideal neural network weights. The uncertain parameters are initialized either randomly or as zeros (see Equation (58)) to test the capability of the control law to compensate for the parametric uncertainty. The neural network estimate is included in the control law to compensate for external disturbances, which could be present under time-varying and uncertain operating conditions. Although the operating conditions of the experimental setup did not exhibit significant external disturbances, the results illustrate the capability to compensate for an inherent weight imbalance in the CMG test bed. The weight imbalance can be observed in the nonzero initial condition of the quaternion error $e_{v1}(0) = -0.15$. This imbalance can be interpreted as an unmodeled, non-vanishing external (gravitational) force. The closed-loop tracking error plots in Fig. 1 demonstrate that the control law significantly reduces the effects of the imbalance by reducing the regulation error $e_{v1}(t)$.

The tracking error plots in Fig. 1 exhibit a slow convergence time, and future work will focus on extending the proposed attitude control law to formally address this issue. The results presented here are intended to demonstrate the ultimate convergence of the quaternion regulation error as proven in the Lyapunov stability analysis (i.e., as mathematically expressed in Inequality (57)).

The neural network utilized to generate these experimental results was designed to adapt online, without the requirement of an offline training phase. The use of online NN adaptation in the control law as opposed to offline training is a primary focus of the NN application here. The NN complexity, as described in terms of the number of hidden-layer neurons (see Equation (58)), was selected based on the desire to achieve the best possible performance in the control task. The NN structure in this result was not optimized to minimize the NN complexity in the proposed attitude control method; this issue will be formally addressed in future research.

## 8. Conclusions

A robust and adaptive NN-based attitude controller is developed for a rigid body satellite. The controller adapts for time-varying satellite inertia properties, parametric uncertainty in the inertia matrix, and input torque uncertainty due to electromechanical disturbances in the CMG gimbal loops. In addition, the NN controller compensates for unmodeled, non-LP external disturbances. In addition, since a singularity robust steering law is incorporated in the control design, the proposed approach avoids the singular torque directions inherent in the dynamics of the four single gimbal CMG cluster. The experimental results demonstrate the capability of the proposed control law to regulate a satellite to a desired pose using gimbal angular velocity commands that are within practical limits. The experiment could be improved by using onboard gyroscopes for angular velocity measurements. Future work will focus on output feedback attitude control of a satellite in the presence of CMG anomalies and other uncertain dynamics.

## Conflict of interest statement

The authors declare that there is no conflict of interest regarding the publication of this paper.

## Appendix A

**Lemma 1.** *The matrix-vector product in Equation (19) can be linearly parameterized as*

$$\left(\frac{d}{dt}J(\delta)\right)\left(\frac{1}{2}r+\tilde{R}\omega_d-\alpha e_v\right)=\Omega_0\dot{\delta}, \tag{59}$$

*where* $\Omega_0(t)\in\mathbb{R}^{3\times 4}$ *denotes a state-dependent matrix containing parametric uncertainty.*

**Proof.** The general form for the symmetric inertia matrix $J(\delta(t))$ can be expressed as

$$J(\delta)=\begin{bmatrix} J_1(\delta) & J_2(\delta) & J_3(\delta)\\ J_2(\delta) & J_4(\delta) & J_5(\delta)\\ J_3(\delta) & J_5(\delta) & J_6(\delta)\end{bmatrix} \tag{60}$$

Since the inertia matrix is a function of $\delta(t)\in\mathbb{R}^4$, the time derivative of the $k$th element of $J(\delta(t))$ for $k=1,\ldots,6$ can be obtained as

$$\frac{d}{dt}J_k(\delta)=\sum_{i=1}^{4}\frac{\partial J_k(\delta)}{\partial\delta_i}\dot{\delta}_i. \tag{61}$$

After using the expressions in (59), (60), and (61), one obtains

$$\left(\frac{d}{dt}J(\delta)\right)\left(\frac{1}{2}r+\tilde{R}\omega_d-\alpha e_v\right)=\begin{bmatrix} \sum_{i=1}^{4}\frac{\partial J_1(\delta)}{\partial\delta_i}\dot{\delta}_i & \sum_{i=1}^{4}\frac{\partial J_2(\delta)}{\partial\delta_i}\dot{\delta}_i & \sum_{i=1}^{4}\frac{\partial J_3(\delta)}{\partial\delta_i}\dot{\delta}_i\\ \sum_{i=1}^{4}\frac{\partial J_2(\delta)}{\partial\delta_i}\dot{\delta}_i & \sum_{i=1}^{4}\frac{\partial J_4(\delta)}{\partial\delta_i}\dot{\delta}_i & \sum_{i=1}^{4}\frac{\partial J_5(\delta)}{\partial\delta_i}\dot{\delta}_i\\ \sum_{i=1}^{4}\frac{\partial J_3(\delta)}{\partial\delta_i}\dot{\delta}_i & \sum_{i=1}^{4}\frac{\partial J_5(\delta)}{\partial\delta_i}\dot{\delta}_i & \sum_{i=1}^{4}\frac{\partial J_6(\delta)}{\partial\delta_i}\dot{\delta}_i\end{bmatrix}\begin{bmatrix} g_1(t)\\ g_2(t)\\ g_3(t)\end{bmatrix} \tag{62}$$

where $g_i(t)\in\mathbb{R}$, for $i=1,2,3$, is the $i$th element of $\left(\frac{1}{2}r+\tilde{R}\omega_d-\alpha e_v\right)\in\mathbb{R}^3$. The expression in (62) can be rewritten as

$$\left(\frac{d}{dt}J(\delta)\right)\left(\frac{1}{2}r+\tilde{R}\omega_d-\alpha e_v\right)= \tag{63}$$
$$\begin{bmatrix} \left(g_1(t)\frac{\partial J_1(\delta)}{\partial\delta_1}\dot{\delta}_1+g_2(t)\frac{\partial J_2(\delta)}{\partial\delta_1}\dot{\delta}_1+g_3\frac{\partial J_3(\delta)}{\partial\delta_1}\dot{\delta}_1\right)+\cdots+\left(g_1(t)\frac{\partial J_1(\delta)}{\partial\delta_4}\dot{\delta}_4+g_2(t)\frac{\partial J_2(\delta)}{\partial\delta_4}\dot{\delta}_4+g_3\frac{\partial J_3(\delta)}{\partial\delta_4}\dot{\delta}_4\right)\\ \left(g_1(t)\frac{\partial J_2(\delta)}{\partial\delta_1}\dot{\delta}_1+g_2(t)\frac{\partial J_4(\delta)}{\partial\delta_1}\dot{\delta}_1+g_3\frac{\partial J_5(\delta)}{\partial\delta_1}\dot{\delta}_1\right)+\cdots+\left(g_1(t)\frac{\partial J_2(\delta)}{\partial\delta_4}\dot{\delta}_4+g_2(t)\frac{\partial J_4(\delta)}{\partial\delta_4}\dot{\delta}_4+g_3\frac{\partial J_5(\delta)}{\partial\delta_4}\dot{\delta}_4\right)\\ \left(g_1(t)\frac{\partial J_3(\delta)}{\partial\delta_1}\dot{\delta}_1+g_2(t)\frac{\partial J_5(\delta)}{\partial\delta_1}\dot{\delta}_1+g_3\frac{\partial J_6(\delta)}{\partial\delta_1}\dot{\delta}_1\right)+\cdots+\left(g_1(t)\frac{\partial J_3(\delta)}{\partial\delta_4}\dot{\delta}_4+g_2(t)\frac{\partial J_5(\delta)}{\partial\delta_4}\dot{\delta}_4+g_3\frac{\partial J_6(\delta)}{\partial\delta_4}\dot{\delta}_4\right)\end{bmatrix}.$$

After factoring out the terms $\dot{\delta}_i(t)$, for $i=1,\ldots,4$, the expression in (63) can be rewritten as

$$\left(\frac{d}{dt}J(\delta)\right)\left(\frac{1}{2}r+\tilde{R}\omega_d-\alpha e_v\right)= \tag{64}$$

$$\begin{bmatrix} \left(g_1(t)\frac{\partial J_1(\delta)}{\partial \delta_1} + g_2(t)\frac{\partial J_2(\delta)}{\partial \delta_1} + g_3\frac{\partial J_3(\delta)}{\partial \delta_1}\right)\dot{\delta}_1 + \cdots + \left(g_1(t)\frac{\partial J_1(\delta)}{\partial \delta_4} + g_2(t)\frac{\partial J_2(\delta)}{\partial \delta_4} + g_3\frac{\partial J_3(\delta)}{\partial \delta_4}\right)\dot{\delta}_4 \\ \left(g_1(t)\frac{\partial J_2(\delta)}{\partial \delta_1} + g_2(t)\frac{\partial J_4(\delta)}{\partial \delta_1} + g_3\frac{\partial J_5(\delta)}{\partial \delta_1}\right)\dot{\delta}_1 + \cdots + \left(g_1(t)\frac{\partial J_2(\delta)}{\partial \delta_4} + g_2(t)\frac{\partial J_4(\delta)}{\partial \delta_4} + g_3\frac{\partial J_5(\delta)}{\partial \delta_4}\right)\dot{\delta}_4 \\ \left(g_1(t)\frac{\partial J_3(\delta)}{\partial \delta_1} + g_2(t)\frac{\partial J_5(\delta)}{\partial \delta_1} + g_3\frac{\partial J_6(\delta)}{\partial \delta_1}\right)\dot{\delta}_1 + \cdots + \left(g_1(t)\frac{\partial J_3(\delta)}{\partial \delta_4} + g_2(t)\frac{\partial J_5(\delta)}{\partial \delta_4} + g_3\frac{\partial J_6(\delta)}{\partial \delta_4}\right)\dot{\delta}_4 \end{bmatrix}.$$

Clearly, the expression in (64) can be rewritten as the matrix vector product

$$\left(\frac{d}{dt}J(\delta)\right)\left(\frac{1}{2}r + \tilde{R}\omega_d - \alpha e_v\right) = \begin{bmatrix} \Omega_{0(1,1)} & \Omega_{0(1,2)} & \Omega_{0(1,3)} & \Omega_{0(1,4)} \\ \Omega_{0(2,1)} & \Omega_{0(2,2)} & \Omega_{0(2,3)} & \Omega_{0(2,4)} \\ \Omega_{0(3,1)} & \Omega_{0(3,2)} & \Omega_{0(3,3)} & \Omega_{0(3,4)} \end{bmatrix} \begin{bmatrix} \dot{\delta}_1 \\ \dot{\delta}_2 \\ \dot{\delta}_3 \\ \dot{\delta}_4 \end{bmatrix} = \Omega_0 \dot{\delta}. \tag{65}$$

In (65), the parallel axis theorem can be used to prove that the elements $\Omega_{0(i,j)}$, for $i = 1, 2, 3$ and $j = 1, 2, 3, 4$, of the matrix $\Omega_0(t)$ contain linear combinations of uncertain constant gimbal inertia parameters and the measurable signals $e_v(t)$, $e_0(t)$, $\omega_d(t)$, $\omega(t)$, and $\delta(t)$. That proof is a straightforward application of the parallel axis theorem and is omitted here for brevity. □

## References


[1] W. MacKunis, K. Dupree, N. Fitz-Coy, W.E. Dixon, Adaptive satellite attitude control in the presence of inertia and CMG gimbal friction uncertainties, J. Astronaut. Sci. 56 (1) (2008) 121–134.
[2] A novel single thruster control strategy for spacecraft attitude stabilization, Acta Astronaut. 86 (2013) 55–67.
[3] Nonlinear $h_\infty$ based underactuated attitude control for small satellites with two reaction wheels, Acta Astronaut. 104 (1) (2014) 159–172.
[4] W.A. Kishore, S. Dasgupta, G. Ray, S. Sen, Control allocation for an over-actuated satellite launch vehicle, Aerosp. Sci. Technol. 28 (1) (2013) 56–71.
[5] T. Inamori, N. Sako, S. Nakasuka, Magnetic dipole moment estimation and compensation for an accurate attitude control in nano-satellite missions, Acta Astronaut. 68 (2011) 2038–2046.
[6] P. Singla, K. Subbarao, J.L. Junkins, Adaptive output feedback control for spacecraft rendezvous and docking under measurement uncertainty, J. Guid. Control Dyn. 29 (4) (2006) 892–902.
[7] B.T. Costic, D. Dawson, M.S. de Queiroz, V. Kapila, A quaternion-based adaptive attitude tracking controller without velocity measurements, J. Guid. Control Dyn. 24 (2001) 1214–1223.
[8] H. Wong, M.S. de Queiroz, V. Kapila, Adaptive tracking control using synthesized velocity from attitude measurements, Automatica 37 (6) (2001) 947–953.
[9] S. Yin, X. Li, H. Gao, O. Kaynak, Data-based techniques focused on modern industry: an overview, IEEE Trans. Ind. Electron. 62 (1) (2015) 657–667.
[10] S. Yin, X. Zhu, O. Kaynak, Improved PLS focused on key-performance-indicator-related fault diagnosis, IEEE Trans. Ind. Electron. 62 (3) (2015) 1651–1658.
[11] K. KrishnaKumar, S. Rickard, S. Bartholomew, Adaptive neuro-control for spacecraft attitude control, Neurocomputing 9 (2) (1995) 131–148.
[12] N. Sadati, N.d. Tehrani, H.R. Bolandhemmat, Multivariable adaptive satellite attitude controller design using RBF neural network, in: Proc. of the IEEE Int'l Conf. on Networking, Sensing and Control, Taipei, Taiwan, March 2004.
[13] C.W. Tan, S. Park, K. Mostov, P. Varaiya, Design of gyroscope-free navigation systems, in: IEEE Int'l Conf. on Intelligent Transportation Systems, 2001, pp. 286–291.
[14] N. Unnikrishnan, S.N. Balakrishnan, R. Padhi, Dynamic re-optimization of a spacecraft attitude controller in the presence of uncertainties, in: Proc. of IEEE Int'l Symposium on Intelligent Control, Munich, Germany, October 2006.
[15] S. Yin, P. Shi, H. Yang, Adaptive fuzzy control of strict-feedback nonlinear time-delay systems with unmodeled dynamics, IEEE Trans. Cybern. PP (99) (2015) 1.
[16] S. Yin, G. Wang, H. Gao, Data-driven process monitoring based on modified orthogonal projections to latent structures, IEEE Trans. Control Syst. Technol. PP (99) (2015) 1–8.
[17] S. Yin, Z. Huang, Performance monitoring for vehicle suspension system via fuzzy positivistic C-means clustering based on accelerometer measurements, IEEE/ASME Trans. Mechatron. 20 (5) (2015) 2613–2620.
[18] C.J. Heiberg, D. Bailey, B. Wie, Precision spacecraft pointing using single-gimbal control moment gyroscopes with disturbance, J. Guid. Control Dyn. 23 (1) (2000).
[19] P. Hughes, Spacecraft Attitude Dynamics, Wiley, New York, 1994.
[20] B. Wie, Space Vehicle Dynamics and Control, AIAA Inc., Reston, VA, 1998.
[21] M. Kaplan, Modern Spacecraft Dynamics and Control, John Wiley and Sons, New York, NY, 1976.
[22] W. Mackunis, K. Dupree, S. Bhasin, W.E. Dixon, Adaptive neural network satellite attitude control in the presence of inertia and CMG actuator uncertainties, in: Proc. American Control Conf., Seattle, WA, June 2008, pp. 2975–2980.
[23] F.L. Lewis, Nonlinear network structures for feedback control, Asian J. Control 1 (4) (1999) 205–228.
[24] Y. Nakamura, H. Hanafusa, Inverse kinematic solutions with singularity robustness for robot manipulator control, J. Dyn. Syst. Meas. Control 108 (3) (1986) 163–171.
[25] N. Bedrossian, J. Paradiso, E. Bergmann, D. Rowell, Steering law designs for redundant SGCMG systems, AIAA J. Guidance & Control 13 (6) (1991) 1083–1089.
[26] F.L. Lewis, A. Yesildirek, K. Liu, Multi-layer neural network controller with guaranteed tracking performance, IEEE Trans. Neural Netw. 7 (2) (1996).
[27] W. Dixon, Adaptive regulation of amplitude limited robot manipulators with uncertain kinematics and dynamics, IEEE Trans. Autom. Control 52 (3) (2007) 488–493.
[28] E. Zergeroglu, W. Dixon, A. Behal, D. Dawson, Adaptive set-point control of robotic manipulators with amplitude-limited control inputs, Robotica 18 (2000) 171–181.